Eleventh International Conference on CFD in the Minerals and Process Industries
CSIRO, Melbourne, Australia
7-9 December 2015

COMPARATIVE ANALYSIS OF TWO MULTIPHASE MODELLING APPROACHES FOR BLOOD FLOW

Mohit P. TANDON[1*], **Jebin ELIAS**[1], **Simon LO**[2]
[1]CD-Adapco India, 4th Floor, Parakh House, 1, Boat Club Road, Pune - 411 001, India
[2]Trident House, Trident Park, Basil Hill Road, Didcot, OX11 7HJ, United Kingdom

[*] Corresponding author, E-mail : mohit.tandon@cd-adapco.com

ABSTRACT

The Euler-Euler methodology implemented in STAR-CCM+ is used for modelling blood flow in narrow tubes. Two particulate flow modelling approaches, one: kinetic theory based granular flow (KTGF), and second: two-fluid theory based suspension rheology, are used to understand the phenomenon behind the migration of red blood cells (RBCs) from the walls to the core in narrow flow channels. It is demonstrated that the stress induced diffusion is responsible for the motion of the RBCs towards the center, and this particle migration phenomenon explains the Fåhræus-Lindqvist effect. The computed haematocrit distribution from the numerical simulations performed agrees with experimental measurements, and both KTGF model and suspension model are able to predict the flow characteristics analogously. But, it is highlighted that by accounting for the inelasticity of the walls, KTGF approach significantly influences and improves the near wall prediction of the haematocrit concentrations.

Keywords : Blood Flow, Two Fluid Model, Kinetic Theory of Granular Flows, Suspensions, Stress induced diffusion.

Nomenclature

Greek Letters

λ	Anisotropy parameter
γ_s	Collisional dissipation rate [kg/(m.s^3)]
ρ	Density [kg/m^3]
η	Dimensionless Viscosity
θ	Granular temperature [m^2/s^2]
φ	Specularity coefficient
ε	Strain rate
τ	Stress Tensor [kg/(m.s^2)]
μ	Viscosity [kg/(m.s)]
α	Volume Fraction

Latin Symbols

A	Interphase momentum coefficient [kg/ (m^3.s)]
F	Force [N]
Q	Normal stress anisotropy tensor
Re	Reynolds Number
$\boldsymbol{c}$	Fluctuating velocity [m/s]
d	Particle diameter [m]
e	Coefficient of restitution
$\boldsymbol{g}$	Gravity [m/s^2]
g_0	Radial Distribution Function
k	Granular conductivity [kg/(m.s)]
n	Normal [m]
p	Pressure [Pa]
$\mathbf{u}$	Velocity [m/s]

Sub/superscripts

NS	normal stress
S	shear stress
b	bulk
i,k	i,k-th phase
int	interaction
l	liquid phase
max	maximum packing limit
p	particle contribution
s	solid phase
$slip$	slip between phases
w	wall

INTRODUCTION

Blood is a rich suspension of red blood cells (RBCs) in Newtonian fluid, plasma. Biophysics of blood flow in micro-vessels has been studied for many years, and it has been known for long now that RBCs in narrow blood vessels migrate away from the wall which leads to a cell-free layer near the wall. This causes the blood viscosity to reduce and causes apparent viscosity of blood to depend on the tube diameter. This phenomena is referred as Fåhræus-Lindqvist effect (1931).

Migration of RBCs from the wall to the core of the blood vessels has been widely studied in the literature. Numerous studies on this effect have been based on multiphase nature of the blood. Nair *et al.* (1989) used a two fluid model for blood in modelling transport of oxygen in arterioles but the study did not account for the dependence of thickness of cell-free layer on the haematocrit concentration. Sharan and Popel (2001) put forward a model with central core of suspended erythrocytes and a cell-free layer surrounding the core. In their study roughness at the interface between the plasma rich annulus and the core is accounted by modelling an increased effective plasma viscosity in the cell-free layer. Jung *et al.* (2006) suggested to model blood flow as a mixture of plasma and RBCs with shear dependent viscosity as an input. Gidaspow and Huang (2009) later theorized the use of kinetic theory based granular flow model (Jenkins and Savage (1983), Lun *et al.* (1984) and Ding and Gidaspow (1990)) for explaining the migration of RBCs from the wall to center in narrow tubes.

On the other hand, Nott and Brady (1994) suggested that the particle contribution to total suspension stress was responsible for the particle migration phenomena seen in suspensions. Morris and Boulay (1999) studied the role of normal stresses in causing this particle migration and macroscopic spatial variation of the particle volume fraction in a mixture of particles suspended in Newtonian fluid. Lhuillier (2009) later proposed that migration of particle relative to the fluid is the result of two different phenomena, first being the inhomogeneity of the stress resulting from direct interparticle forces and second being the Fick-like hydrodynamic force acting on the particles.

Boyer *et al.* (2011) extensively studied the rheology of dense suspensions to show that they exhibit a behaviour similar to granular media. This motivates the study presented in this article, wherein results from two radically different approaches for modelling particulate flow, kinetic theory based granular model and suspension rheology based two-fluid model as implemented in STAR-CCM+ are compared, with an objective to acquire a deeper understanding of particle migration commonly observed. A clear understanding of RBCs migration in narrow blood vessels is expected to be very useful for several medical applications. For both the modelling approaches used in this study, blood viscosity is not an input into the model but is modelled via correlations appropriate to the method used.

MODEL DESCRIPTION

The Euler-Euler model in STAR-CCM+ treats the different phases as inter-penetrating continua with phase dependent velocity, temperature and other flow properties (Tandon *et al.*, 2013). One such phase dependent continuous function is volume fraction, which defines the percentage of the volume occupied by each individual phase. Conservation equations for these quantities are solved for each phases, and additional closure laws are defined to model the interactions between the phases.

STAR-CCM+ solves conservation equations for mass and momentum for each phase i in the following form :

Continuity

$$\frac{\partial}{\partial t}\alpha_i\rho_i + \nabla\cdot\alpha_i\rho_i\mathbf{u_i} = 0 \tag{1}$$

Momentum equation for i^{th} phase :

$$\frac{\partial}{\partial t}\alpha_i\rho_i\mathbf{u_i} + \nabla\cdot\alpha_i\rho_i\mathbf{u_i}\mathbf{u_i} = -\alpha_i\nabla p + \alpha_i\rho_i\mathbf{g} + \nabla\cdot\tau_i + F_{int,ik} \tag{2}$$

Shear stress τ, is modelled as,

$$\tau_i = \alpha_i\mu_i\left(\nabla\mathbf{u_i} + (\nabla\mathbf{u_i})^T - \frac{2}{3}\nabla\cdot\mathbf{u_i}\right) \tag{3}$$

Interface momentum transfer, $F_{int,ik}$, represents the force balance incorporating the sum of all the forces each phase exert on each other. The only interaction force used in this study is the drag force, which is modelled by using the Gidaspow drag correlation (Bouillard *et al.* (1989)) which in turn, uses Wen and Hu (1966) correlation for particle concentration below 0.2 and Ergun's equation beyond it.

$$F_{int,ik} = A_D\left(\mathbf{u_i} - \mathbf{u_k}\right) \tag{4}$$

with

$$A_D = \begin{cases} \frac{150\alpha_d^2\mu_c}{\alpha_c d_s^2} + \frac{1.75\alpha_d\rho_c|\mathbf{v_r}|}{d_s} & : \alpha_d \geq \alpha_{tr} \\ \frac{3}{4}C_D.\frac{\alpha_d\rho_c}{d_s^2}.\left|\mathbf{v_r}\right|\alpha_c^{-1.65} & : \alpha_d < \alpha_{tr} \end{cases} \tag{5}$$

where, the Drag Coefficient C_D for spherical rigid particles is computed based on the Schiller and Naumann (1933) correlation as :

$$C_D = \begin{cases} \frac{24}{Re_d}.\left(1+0.15Re_d^{0.687}\right) & : \quad 0 < Re_d \leq 1000 \\ 0.44 & : \quad Re_d > 1000 \end{cases} \tag{6}$$

Granular Flow Model

With granular stress model being used for particulate phase, τ_s, is modeled as,

$$\tau_s = -p_s + \mu_s\left(\nabla\mathbf{u_s} + (\nabla\mathbf{u_s})^T + \left(\mu_{b,s} - \frac{2}{3}\right)\nabla\cdot\mathbf{u_s}\right) \tag{7}$$

where, p_s is the solid pressure force representing the normal force due to the interactions between the particle and prevents the particles from packing beyond the maximum packing limit. Lun *et al.* (1984) model this as a function of granular temperature represented as below :

$$P_s = \alpha_s\rho_s\theta_s(1+2(1+e)\alpha_s g_0) \tag{8}$$

KTGF implementation in STAR-CCM+ as detailed by Tandon and Karnik (2014) determines the fluidic properties of the particulate phase by accounting for the in-elasticity of the particles and postulates that solid viscosity and the solid stress are functions of granular temperature. Granular temperature, θ_s, is defined based on fluctuations in solid phase velocity, c_s as:

$$\theta_s = \frac{1}{3} < \mathbf{c_s}\mathbf{c_s} > \tag{9}$$

KTGF further introduces a conservative form of transport equation for granular temperature which is given as,

$$\frac{3}{2}\left[\frac{\partial}{\partial t}\alpha_s\rho_s\theta_s + \nabla\cdot\alpha_s\rho_s\theta_s\mathbf{u_s}\right] = \underbrace{\tau_{s,k}:\nabla\mathbf{u_s}}_{\text{Production (P)}} \underbrace{+\nabla\cdot k_s\nabla\theta_s}_{\text{Diffusion }(D_{fluctuating})} \underbrace{-\gamma_s}_{\text{Dissipation }(D_{collisions})} \tag{10}$$

P : Production of fluctuating energy due to shear in the particle phase

$D_{fluctuating}$: Diffusion of fluctuating energy along gradients in granular temperature

$D_{collisions}$: Dissipation due to inelastic collisions

The dissipation of granular energy (fluctuating energy), γ_s, due to inelastic particle - particle collisions is modelled in this study as in Lun *et al.* (1984). Their work omitted the term accounting for $\nabla.\mathbf{u_s}$ which was included in the form originally proposed by Jenkins and Savage (1983).

$$\gamma_s = 12(1-e^2)\frac{\alpha_s^2 \rho_s g_0}{d_s\sqrt{\pi}}\theta_s^{3/2} \tag{11}$$

Radial distribution function, g_0, is an estimate of particle pair density at a distance equivalent to the particle diameter. It increases with increasing particle volume fraction. In this study, we used the expression by Ding and Gidaspow (1990),

$$g_0 = \frac{3}{5}\left[\left(1-\frac{\alpha_s}{\alpha_{s,max}}\right)^{1/3}\right]^{-1} \tag{12}$$

The radial distribution function is written as a Taylor series approximation at high volume fractions close to maximum packing. The expression in equation 12 was numerically blended with Taylor series expression to avoid convergence difficulties.

Suspension Model

The suspension model in STAR-CCM+ uses a stress form which accounts for particle contribution to the total stress in suspensions.

Morris and Boulay (1999) indicate that anisotropic compressive normal stresses are present in sheared suspensions. Their study proposes a rheological model for suspensions which includes normal stresses as the particle contribution to the total suspension stress. Following their work, the particle contribution to the total suspension stress is modeled as:

$$\begin{aligned}\tau_p &= \tau_{p,NS} + \tau_{p,S} \\ &= -\mu_l \eta_n(\alpha)\varepsilon Q + 2\mu_l \eta_p(\alpha) D\end{aligned} \tag{13}$$

where, ε is the local strain rate, D is the local strain rate tensor, and, Q is the material dependent anisotropic tensor :

$$Q = \begin{pmatrix}\lambda_1 & 0 & 0 \\ 0 & \lambda_2 & 0 \\ 0 & 0 & \lambda_3\end{pmatrix} \tag{14}$$

λ_1, λ_2 and λ_3 are the anisotropy parameters which should be positive. Anisotropy can be augmented in the direction of the local flow by using appropriate values for λ_1, λ_2 and λ_3. η_n and η_p are the dimensionless normal and shear viscosities which are modelled as proposed by Morris and Boulay (1999):

$$\begin{aligned}\eta_p = \; & 2.5\alpha_s\left(1-\tfrac{\alpha_s}{\alpha_{s,max}}\right)^{-1} + \\ & K_s\left(\tfrac{\alpha_s}{\alpha_{s,max}}\right)^2\left(1-\tfrac{\alpha_s}{\alpha_{s,max}}\right)^{-2}\end{aligned} \tag{15}$$

and

$$\eta_n = K_n\left(\frac{\alpha_s}{\alpha_{s,max}}\right)^2\left(1+\frac{\alpha_s}{\alpha_{s,max}}\right)^{-2} \tag{16}$$

This model is adopted within the two-phase model framework based on the theory proposed by Lhuillier (2009). Additional details on it can be found in STAR-CCM+ documentation (CD-adapco, 2014).

COMPUTATIONAL INVESTIGATION

This investigation was carried out in the commercial CFD code STAR-CCM+ from CD-adapco. The code uses PC-SIMPLE (Vasquez and Iranov, 2000) for pressure-velocity coupling. The code solves the velocity components of all phases together in a segregated manner, and the pressure correction equation is based on the continuity equation.

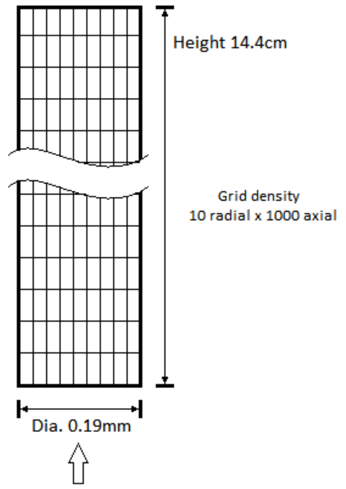

Figure 1: Schematic of the Flow column

Taylor (1955) experimentally collected extensive data for the RBCs concentration for flows through narrow tubes for several different RBC concentration levels. This data forms the basis of this current investigation. The physical dimensions and specifications of the narrow tube used by Taylor for the experiments is given in Table 1. The RBCs along with blood plasma flow into the channel and the data collected from a PIV measurement apparatus was used to estimate the concentration of the RBCs cells in the tube, and the effective holdup.

Simulations were performed for two volume fraction conditions (haematocrit concentrations) : $\alpha_s = 0.24$ and $\alpha_s = 0.57$ with a parabolic inlet velocity with the maximum velocity at $0.2m/s$. The 2D computational domain of uniform 10,000 cells (10 radial and 1000 axial) was used for the study. Figure 1 shows the schematic of the column geometry and the boundary conditions, and table 1 gives the relevant dimensions of the flow channel and the simulation conditions.

All the simulations use second order convection scheme for volume fraction, velocity and granular temperature. Time step of 10^{-3}s was used for all the simulations and they were run for 10.0s. The time averaged distributions of flow variables were computed for period of 4.0 - 10.0s. The start time of 4.0s ensures that the time averaging is performed only after the flow in the column has attained a quasi-steady state.

Boundary Conditions

Dirichlet boundary condition was used for liquid phase at the inlet of the channel with pressure outlet boundary condition for the top boundary. The pressure is specified as 80.0 mm Hg, at the top boundary.

When using granular theory, no-slip boundary conditions is used at the side-walls for the plasma and partial-slip boundary condition as proposed by Johnson and Jackson (1987) is used for the RBCs. The Johnson and Jackson wall treatment

Tube diameter	0.19mm
Tube Length	14.4 cm
Plasma density	1020.0 kg/m^{-3}
Plasma viscosity	0.0012 kg.m^{-1}s^{-1}
RBC size	8μm
RBC density	1092 kg/m^{-3}
Pressure head	80 mm Hg
Grid density	10 radial and 1000 axial
Time step	1.0$\times$10^{-3}s

Table 1: Simulation parameters

for the granular temperature enforces the following criterion at the boundary :

$$\mathbf{u}_{\mathbf{s},\mathbf{w}} = -\frac{6\alpha_s\mu_s}{\sqrt{3\theta_s}\pi\phi\rho_s\alpha_s\mathbf{g_o}}.\frac{\partial \mathbf{u}_{\mathbf{s},\mathbf{w}}}{\partial n} \tag{17}$$

$$\theta_{s,w} = -\frac{k\theta_s}{\gamma_w}\frac{\partial \theta_{s,w}}{\partial n} + \frac{\sqrt{3}\pi\phi\rho_s\alpha_s\mathbf{u}_{\mathbf{s},\mathbf{slip}}{}^2\mathbf{g_o}\theta_s^{3/2}}{6\alpha_{s,max}\gamma_w} \tag{18}$$

where, γ_w, is expressed in term of particle-wall restitution coefficient, e_w, as

$$\gamma_w = \frac{\sqrt{3}\pi(1-e_w^2)\alpha_s\rho_s\mathbf{g_o}\theta_s^{3/2}}{4\alpha_{s,max}} \tag{19}$$

The equation 18 represents the granular energy conducted to the wall after accounting for the generation of granular energy due to particle slip at the wall and the dissipation of granular energy due to inelastic collisions between the particles and the wall.

Simulations using suspension theory used no-slip boundary condition for plasma at the walls. However, both slip and no-slip boundary conditions were used for the particulate phase (RBCs) for the different analysis performed, and is specified in the respective sections where required.

RESULTS & DISCUSSION

This section is divided into three parts, the first, comparing the results from simulation using granular and suspension theories respectively, second discussing the role of particle-wall modelling when using granular theory and the third discussing the role of normal stress and wall treatment for RBCs when using suspension theory.

When comparing the results from two different theories it was noted that both successfully predict the migration of RBCs to the center of blood vessel as demonstrated in by Figures 2 and 3 which plot the RBCs distribution radially along the tube for $\alpha_s = 0.24$ and 0.57 respectively thereby confirming Fåhræus-Lindqvist effect. However it can be seen that granular theory successfully predicts the small increase in RBCs concentration near the wall, a trend observed in the measurements recorded by Taylor (1955) as well.

Computed time averaged RBC axial velocities are compared in Figure 4 where it has been shown that both the modelling approaches predicts a parabolic distribution for the axial velocity of the RBC.

It can also be deduced from Figures 2 and 3 that particle-wall interactions play stronger role when RBC concentration is

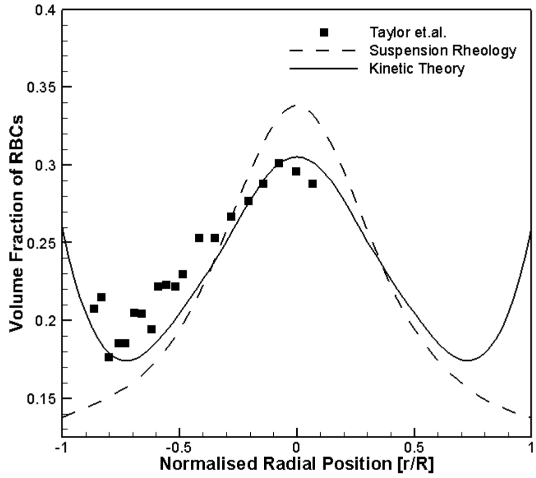

Figure 2: Volume Fraction of RBCs compared against the experimental data for both kinetic theory, and suspension modelling approach for RBC concentration = 24 %.

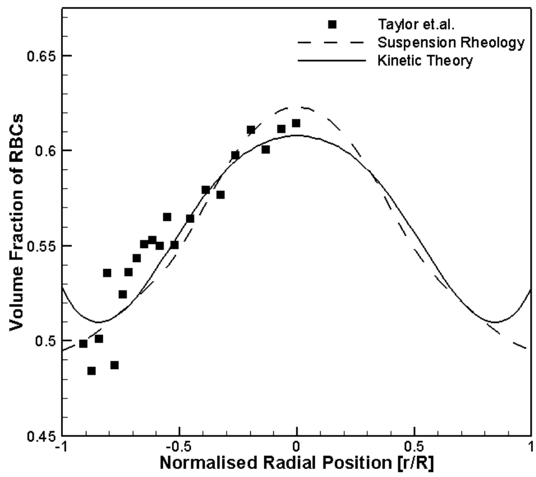

Figure 3: Volume Fraction of RBCs compared against the experimental data for both kinetic theory, and suspension modelling approach for RBC concentration = 57 %.

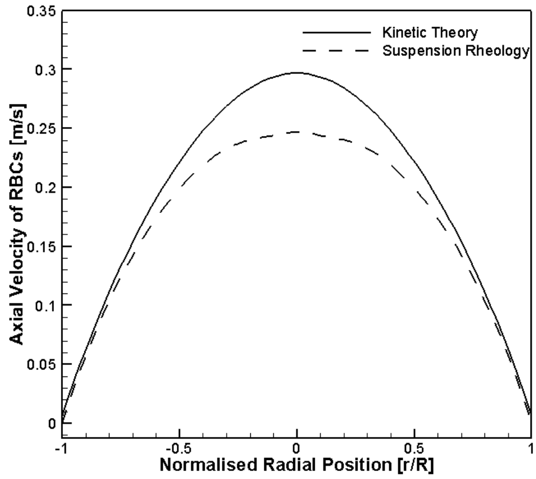

Figure 4: Axial velocity of RBCs for both kinetic theory, and suspension modelling approach.

24% by volume. This is consistent with Lazaro *et al.* (2014) who suggested that at lower concentration of cells in narrow vessels dynamics of flow is dominated by particle-wall distributions and role of non-linearities induced in the rheology of the blood due to cell deformations is more relevant in thick tubes.

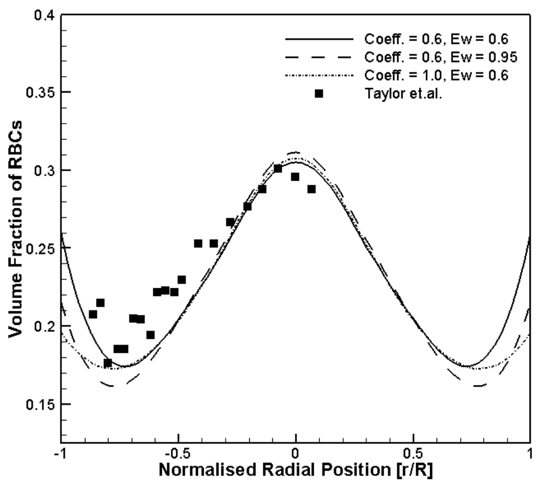

Figure 5: Particle wall modelling : Radial variation of volume fraction of RBCs.

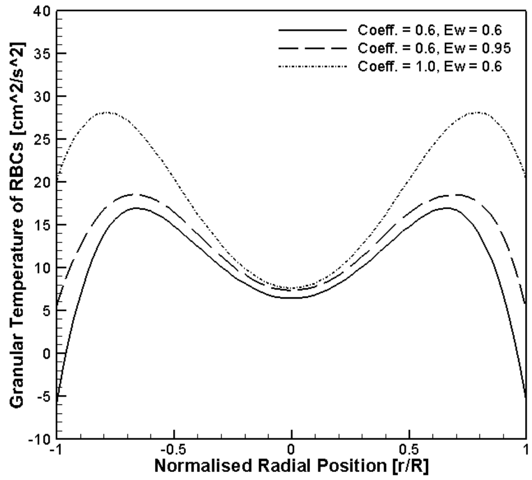

Figure 6: Particle wall modelling : Radial variation of Granular Temperature of RBCs.

In second part we evaluate the role of particle-wall modelling. Figures 5 and 6 compare the results from simulations using e_w = 0.95 and 0.6 in Johnson-Jackson boundary condition when using a specularity values of 0.6. The results for a case using specularity value of 1.0 with e_w = 0.6 are also added for evaluating the role of dissipation of granular energy near the walls. It must be noted that specularity coefficient is indicative of fraction of collisions that transfer momentum to the wall.

In all the simulations, particle-particle coefficient of restitution is set at 0.95. We assume particle-particle coefficient of restitution at 0.95 throughout this study. The coefficient of restitution for a system is a modelling parameter and is unknown. By using low value for particle-wall coefficient of restitution in problem set-up, an attempt is made to mimic the dissipation due to the partially flexible tube. Figure 5 illustrates that the near wall prediction is better for case with particle-wall coefficient of restitution set at 0.6 and specularity value of 0.6. This can be explained by evaluating the granular temperature profiles for corresponding simulations in Figure 6. It can be seen that granular temperature decreases more near wall in case using value of 0.6 for particle-wall coefficient of restitution. The profile of granular temperature explains the migration of particles towards the core and also the small increase in particle concentration near the walls, as particles tend to migrate away from regions of high granular energy to region of low granular energy, which is captured by the normal particle stress term arising due to the inter-particle interactions.

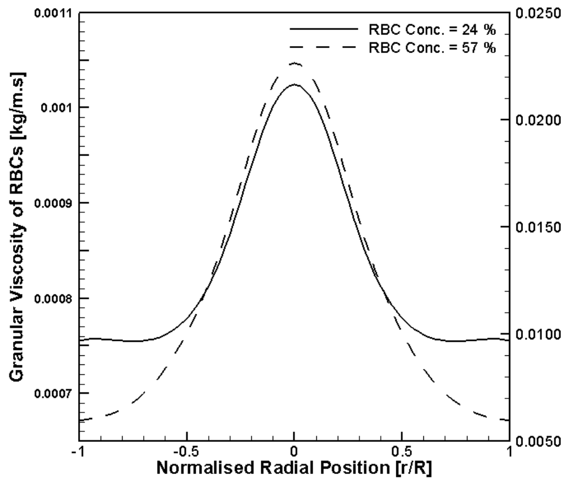

Figure 7: Radial variation of Granular Viscosity.

Figure 7 represents the granular viscosity distribution along the radius of the tube. It uses the formulation from (Gidaspow, 1994) to compute the solid viscosity from granular temperature. The plot depicts higher viscosity in the core of the tube and is in agreement with previous works from Pries *et al.* (1992) and Gidaspow and Huang (2009). The observed trend is attributed to higher RBC concentrations near the core.

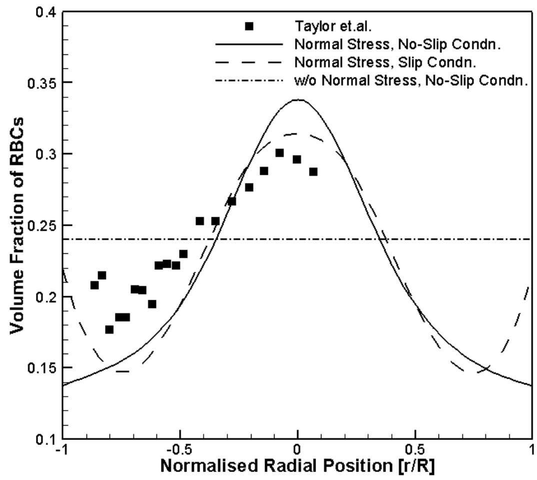

Figure 8: Difference in the volume fraction profile of RBCs depending on the usage of normal stress term in Suspension modelling method.

For the third part, we run two cases one with normal stress contribution enabled for total suspension stress and other without it. It can be seen from Figure 8 that only when normal stress contribution is enabled particle migrate towards core of the tube. This is consistent with observation of Morris and Boulay (1999). It was observed that the choice of the anisotropy parameters (λ) does not have a significant impact on the final particle distribution.

It is also seen that when using slip boundary condition for RBCs, simulations do predict the increase in concentration of RBCs near the wall but the predicted increase is much higher in comparison with the experimental findings. This indicates that probable partial-slip treatment for RBCs at wall would be more appropriate modelling. However, such an option is not available within STAR-CCM+ with rheology model.

CONCLUSIONS

The study makes successful comparison of results from two different multiphase approaches in modelling blood flow in narrow tubes.

Both theories strongly establish the fact that the *stress induced diffusion* is responsible for the migration of RBCs towards the core of the channel thereby leading to the peak of viscosity in the core of the channel, a phenomenon known as the Fåhræus-Lindqvist effect. However, the variation in the apparent viscosity of blood with respect to the vessel diameter was not studied. A future study focusing on this aspect would be immensely useful in developing deeper understanding of the rheological aspects of blood flow in micro-vessels.

It is seen that the near wall results are more accurate when using KTGF theory which can be attributed to the usage of Johnson-Jackson boundary conditions with granular theory which allows to account for the inelasticity of the particle-wall collisions. The suspension modelling methodology does not allow to control the degree of momentum dissipation near the walls, though the results in this study highlight that a future study into advanced wall treatment relevant to suspension modelling could allow to improve the near wall results for the suspension model.

REFERENCES

BOUILLARD, J.X., LYCZKOWSKI, R.W. and GIDASPOW, D. (1989). "Porosity distributions in a fluidized bed with an immersed obstacle". *AIChE Journal*, **35(6)**, 908–922.

BOYER, F., GUAZZELLI, É. and POULIQUEN, O. (2011). "Unifying suspension and granular rheology". *Phys. Rev. Lett.*, **107**, 188301.

CD-ADAPCO (2014). "STAR-CCM+ documentation". Melville, New York.

DING, J. and GIDASPOW, D. (1990). "A bubbling fluidization model using kinetic theory of granular flow". *AIChE Journal*, **36(4)**, 523–538.

FÅHRÆUS, R. and LINDQVIST, T. (1931). "The viscosity of the blood in narrow capillary tubes". *American Journal of Physiology – Legacy Content*, **96(3)**, 562–568.

GIDASPOW, D. (1994). *Multiphase Flow and Fluidization*. Academic Press, San Diego.

GIDASPOW, D. and HUANG, J. (2009). "Kinetic theory based model for blood flow and its viscosity". *Annals of Biomedical Engineering*, **37(8)**, 1534–1545.

JENKINS, J.T. and SAVAGE, S. (1983). "A theory for the rapid flow of identical, smooth, nearly elastic, spherical particles". *Journal of Fluid Mechanics*, **130**, 187–202.

JOHNSON, P. and JACKSON, R. (1987). "Frictional-collisional constitutive relations for granular materials, with application to plane shearing". *Journal of Fluid Mechanics*, **176**, 67–93.

LAZARO, G.R., HERNANDEZ-MACHADO, A. and PAGONABARRAGA, I. (2014). "Rheology of red blood cells under flow in highly confined microchannels. ii. effect of focusing and confinement". *Soft Matter*, **10**, 7207–7217.

LHUILLIER, D. (2009). "Migration of rigid particles in non-brownian viscous suspensions". *Physics of Fluids*, **21(2)**.

LUN, C., SAVAGE, S., JEFFREY, D. and CHEPURNIY, N. (1984). "Kinetic theories for granular flow: inelastic particles in couette flow and slightly inelastic particles in a general flow field". *Journal of Fluid Mechanics*, **140**, 223–256.

MORRIS, J.F. and BOULAY, F. (1999). "Curvilinear flows of noncolloidal suspensions: The role of normal stresses". *Journal of Rheology*, **43(5)**, 1213–1237.

NAIR, P.K., HELLUMS, J. and OLSON, J. (1989). "Prediction of oxygen transport rates in blood flowing in large capillaries". *Microvascular Research*, **38(3)**, 269 – 285.

NOTT, P.R. and BRADY, J.F. (1994). "Pressure-driven flow of suspensions: simulation and theory". *Journal of Fluid Mechanics*, **275**.

PRIES, A.R., NEUHAUS, D. and GAEHTGENS, P. (1992). "Blood viscosity in tube flow: Dependence on diameter and hematocrit". *The American journal of physiology*, **263**, 1170–1778.

SCHILLER, L. and NAUMANN, A.Z. (1933). "Uber die grundlegenden berechnungen bei der schwerkraftaufbereitung". *Ver. Deut. Ing.*, **77**, 318–320.

SHARAN, M. and POPEL, A. (2001). "A two-phase model for flow of blood in narrow tubes with increased effective viscosity near the wall". *Biorheology*, **38**, 415–428.

TANDON, M.P., KHANOLKAR, A., SPLAWSKI, A. and LO, S. (2013). "Validation of numerical simulations of gas-liquid systems in a vertical pipe". *International Conference on Multiphase Flow*.

TANDON, M. and KARNIK, A. (2014). "Simulation of rectangular fluidized bed with Geldart D particles". *Proc. 10th International Conference on CFD in Oil & Gas, Metallurgical and Process Industries, SINTEF, Trondheim, Norway*.

TAYLOR, M. (1955). "The flow of blood in narrow tubes II. the axial stream and its formation, as determined by changes in optical density". *Australian journal of Experimental Biology*, **33**, 1–16.

VASQUEZ, S.A. and IRANOV, V.A. (2000). "A phase coupled method for solving multiphase problems in unstructured meshes".

WEN, C.Y. and HU, Y. (1966). "Mechanics of fluidization". *Chemical Engineering Progress*, **62(2)**, 100–111.

